Research Article / Mechanical – Materials Engineering http://dx.doi.org/10.15446/ing.investig.v40n2.83893

Alkali-activated concretes based on fly ash and blast furnace slag: Compressive strength, water absorption and chloride permeability

Concretos álcali-activados basados en cenizas volantes y escorias siderúrgicas de alto horno: resistencia a compresión, absorción de agua y permeabilidad a cloruros

Daniela E. Angulo-Ramírez[1], William G. Valencia-Saavedra[2], and Ruby Mejía de Gutiérrez[3]

ABSTRACT

Concretes based on alkali-activated binders have attracted considerable attention as new alternative construction materials, which can substitute Portland Cement (OPC) in several applications. These binders are obtained through the chemical reaction between an alkaline activator and reactive aluminosilicate materials, also named precursors. Commonly used precursors are fly ash (FA), blast furnace slag (GBFS), and metakaolin. The present study evaluated properties such as compressive strength, rate of water absorption (sorptivity), and chloride permeability in two types of alkali-activated concretes (AAC): FA/GBFS 80/20 and GBFS/OPC 80/20. OPC and GBFS/OPC* concretes without alkali-activation were used as reference materials. The highest compressive strength was observed in the FA/GBFS concrete, which reported 26,1% greater strength compared to OPC concrete after 28 days of curing. The compressive strength of alkali-activated FA/GBFS 80/20 and GBFS/OPC 80/20 was 61 MPa and 42 MPa at 360 days of curing, respectively. These AAC showed low permeability to the chloride ion and a reduced water absorption. It is concluded that these materials have suitable properties for various applications in the construction sector.

Keywords: alkaline activated concrete, fly ash, blast furnace slag, mechanical and permeability properties.

RESUMEN

Los concretos basados en cementantes activados alcalinamente han atraído una atención considerable como nuevos materiales de construcción alternativos que pueden sustituir al cemento Portland (OPC) en diferentes aplicaciones. Estos cementantes se obtienen de la reacción química entre un activador alcalino y materiales aluminosilicatos reactivos, también denominados precursores. Los precursores más habituales son cenizas volantes (FA), escoria de alto horno (GBFS) y metacaolin. El presente estudio evaluó propiedades tales como la resistencia a la compresión, la velocidad de absorción de agua (succión capilar) y la permeabilidad a cloruros de dos tipos de concreto activados alcalinamente (AAC): FA/GBFS 80/20 y GBFS/OPC 80/20. Como materiales de referencia se usaron los concretos OPC y GBFS/OPC*. La mayor resistencia a la compresión se observó en el concreto FA/GBFS, que reportó una resistencia 26,1 % mayor en comparación con el concreto OPC después de 28 días de curado. La resistencia a la compresión de los concretos álcali-activados FA/GBFS 80/20 y GBFS/OPC 80/20 fue de 61 MPa y 42 MPa a los 360 días de curado respectivamente. Estos AAC mostraron una baja permeabilidad al ion cloruro y una absorción de agua reducida. Se concluye que estos materiales presentan propiedades que son adecuadas para diversas aplicaciones en el sector de la construcción.

Palabras clave: concretos de activación alcalina, cenizas volantes, escoria siderúrgica de alto horno, propiedades mecánicas y de permeabilidad.

Received: December 3rd, 2019
Accepted: July 6th, 2020

Introduction

Portland cement, with an annual production of almost 3 Gt, has become a prevalent material in the construction industry (Juenger, Winnefeld, Provis, and Ideker, 2011; Gao, Shen, Shen, Liu, and Chen, 2016). However, the cement industry is deemed responsible of producing approximately

[1]Materials Engineer, Universidad del Valle, Colombia. Ph.D. Materials Engineering, Universidad del Valle, Colombia. Composites Materials Group (CENM), Universidad del Valle, Colombia.
E-mail: daniela.eugenia.angulo@correounivalle.edu.co
[2]Materials Engineer, Universidad del Valle, Colombia. Ph.D. Materials Engineering, Universidad del Valle, Colombia. Composites Materials Group (CENM), Universidad del Valle, Colombia.
E-mail: william.gustavo.valencia@correounivalle.edu.co
[3]Chemistry, Universidad del Valle, Colombia. Ph.D. Chemical Science, Universidad Complutense, Madrid, España. Professor, Composites Materials Group (CENM), Universidad del Valle, Colombia.
E-mail: ruby.mejia@correounivalle.edu.co

How to cite: Angulo-Ramírez, D. E., Valencia-Saavedra, W. G., and Mejía de Gutiérrez, R. (2020). Alkali-activated concretes based on fly ash and blast furnace slag: Compressive strength, water absorption and chloride permeability. *Ingeniería e Investigación*, *40*(2), 72-80. 10.15446/ing.investig.v40n2.83893

2 billion tons/year of CO_2 (Qu, Martin, Pastor, Palomo, and Fernández-Jiménez, 2016), amounting 5% to 7% of the global emissions of anthropogenic CO_2 (Zhang, Han, Yu, and Wei, 2018). Projections for the global demand of Portland cement predict that, within the next 40 years, there will be a two-fold increase in production, reaching 6 Gt/year (Gartner, 2004; Taylor, Tam, and Gielen, 2006). Furthermore, according to Zhang et al. (2018), demand generally exceeds projections, as it occurred in 2010. Thus, it is imperative to act now to reduce any CO_2 emissions related to cement production. This has motivated the scientific community and cement producers to work on different alternatives, which include new raw materials, friendlier production processes, less polluting fuels, an increase in structure lifetime, and the development of new types of cement, among other areas of research activity.

Among the new types of cement, those produced through alkaline activation of aluminosilicate precursors, such as fly ash or metakaolin, which use a chemical activator (e.g., silicates, hydroxides, sulphates or carbonates of sodium, or potassium), emerge as a viable alternative because they offer materials with a low environmental impact. So far, research carried out in the field of alkali-activated cements has shown that these materials generate mechanical and durability properties similar or even superior to those of Portland cements (Pacheco-Torgal, Castro-Gomes and Jalali, 2008a; 2018b; Weil, Dombrowski and Buchawald, 2009; Reddy, Edouard, Sobhan, and Tipnis 2011; Bernal, Mejía de Gutiérrez and Provis, 2012; Pereira et al., 2015; Valencia-Saavedra, Angulo and Mejia de Gutiérrez, 2016; Robayo, Mulford, Munera and Mejía de Gutiérrez, 2016; Tennakoon, Shayan, Sanjayan and Xu, 2017). However, the properties of alkali-activated concretes depend on the type of precursor, the amount and concentration of the alkaline solution used as activator, and the curing temperature. Aluminosilicate precursors with high calcium content are associated with the formation of an Al-substituted C-S-H (C-(A)-S-H) gel, while the reaction product of a precursor with low calcium content is a N-A-S-H gel (Na_2O-Al_2O_3-SiO_2-H_2O) with a three-dimensional structure.

Manjunatha, Radhakrishna, Venugopal, and Maruthi (2014), studied the mechanical behavior of FA/GBFS-based alkali-activated concretes cured at room temperature. The authors reported superior mechanical properties compared to OPC-based concrete. Chi (2016) found a similar behavior and reported high compressive strength at an early age, thus surpassing OPC concrete. Other authors have identified that FA/GBFS-based alkali-activated concretes have a high performance when exposed to aggressive environments (Valencia-Saavedra et al., 2016; Valencia-Saavedra and Mejia de Gutierrez, 2017; Valencia-Saavedra, Mejia de Gutierrez and Puertas, 2020).

Aliabdo, El-Moaty, and Emam (2019) found in 100% GBFS-based alkali-activated concretes that about 90% of its compressive strength and tensile strength was reached at 7 days of curing. These resistances are associated with its low porosity. Abubakr, Soliman, and Diab (2020) evaluated the impact performance of the same type of concrete using different modules of activator solution (Ms= SiO_2/Na_2O ratio) and percentages of Na_2O. They reported that, in comparison with OPC, alkali-activated systems generally had up to 70% and 40% better compressive and tensile strength, respectively. Ms of 1,5 increases the impact energy absorption up to 75%. This agrees with Puertas et al. (2018). Bilim and Atis (2012) -using alkali-activated mortars (GBFS/OPC) with 20%, 40%, 60%, 80% and 100% GBFS, Ms = 0,75, as well as sodium concentrations of 4, 6, and 8%- demonstrated that flexure and compressive strength increase with the GBFS percentage and the concentration of the activator. However, the 100% GFBS-based alkali-activated concretes presented the highest compressive strength. Studies have indicated similar behaviors in GBFS-based alkali-activated systems (Rashad, 2013; Lübeck, Gastaldini, Barin and Siqueira, 2012; Noorliyana et al., 2013). However, these authors used 50% GBFS in OPC-based materials and 70-90% GBFS in binary mixtures with MK and FA. Given the above-mentioned properties, these alkaline-activated cements could partially or totally replace Portland cement in many engineering applications. Among the advantages of this type of cement is the fact that they do not require elevated temperatures for processing because the reactions can typically be carried out at room temperature (Bakharev, Sanjayan and Cheng, 1999; Gebregziabiher, Thomas and Peethamparan, 2015).

In the present study, compressive strength, rate of water absorption (sorptivity), and chloride permeability of two types of alkaline activated concretes (AAC) produced from blast furnace slag and fly ash were evaluated. The results were compared with those of a conventional concrete based on Portland cement (OPC) and a blended cement (GBFS/OPC) without alkaline activation, identified as GBFS/OPC* in the present study. The AAC were: FA/GBFS 80/20, and GBFS/OPC 80/20 which can be classified as alkali-activated blended concretes. It is noted that FA presents a high unburned content (20,67%), which restricts its use in Portland cement-based applications.

Materials and experimental methodology

Materials

The materials used in this study were fly ash (FA), granulated blast furnace slag (GBFS), and Colombian ordinary Portland cement (OPC) for general use. The chemical composition and physical characteristics of these materials are shown in Table 1. The Portland cement used in this work contains an addition of limestone that is related to the loss on ignition percentage found in the chemical composition. There is also a high loss on ignition (LOI) of the fly ash component (20,67%), a value that exceeds the 6% that the ASTM C618 (ASTM International, 2019) recommends for the use of pozzolanic supplementary materials in mixtures with Portland cement. The blast furnace slag used is basic and features a good hydraulic behaviour, according to the indices established by different authors (Hadjsadok, Kenai, Courard, Michel and Khatib, 2012; Pal, Mukherjee and Pathak, 2003; Puertas, 1993; Tänzer, Buchwald and Stephan, 2015).

Table 1. Chemical composition and Particle size of the raw materials

Chemical composition (%)	OPC	GBFS	FA
SiO_2	19,13	31,99	28,53
Al_2O_3	4,42	14,54	19,18
Fe_2O_3	4,32	1,12	8,80
CaO	57,70	46,87	6,68
MgO	1,60	1,05	2,24
SO_3	2,32	0,82	–
Loss on Ignition, LOI	9,78	1,80	20,67
Physical characteristic:			
Average Particle Size (μm)	16,07	7,53	18,00

Source: Authors

The XRD diffractograms of the materials used in this research (OPC, GBFS, and FA) are presented in Figure 1. Regarding the OPC, crystalline phases proper to this kind of cement were found: tricalcium silicate (C_3S), tricalcium aluminate (C_3A), dicalcium silicate (C_2S), and gypsum (Y). As for the blast furnace slag, crystalline phases were observed such as calcite (C), quartz (Q), and gehlenite (G), as well as an amorphous halo between 22-36° 2μ. Fly ash reported the presence of Q, Mullite (M), hematite (H), anhydrite (A), and analcime (An), without any evidence of an amorphous phase.

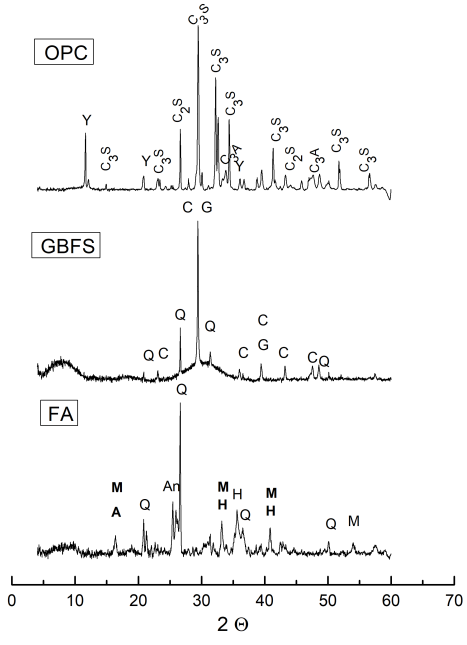

Figure 1. Mineralogical composition of the raw materials based on X-ray diffraction (XRD). Q: quartz, M: mullite, H: hematite, A: anhydrite, An: analcime, C3 S: tricalcium silicate, C3 A: tricalcium aluminate, C2 S: dicalcium silicate, Y: gypsum, C: calcite, and G: gehlenite.
Source: Authors

Design and preparation of concretes

Four types of concrete were manufactured, two as reference, OPC (100%) and GBFS blended concretes (GBFS/OPC* - 80/20); and two alkali-activated concretes (GBFS/OPC 80/20 and FA/GBFS 80/20). The activator used was a mixture of sodium hydroxide (NaOH) and sodium silicate (Na_2SiO_3: SiO_2 = 32,09%, Na_2O = 11,92%, H_2O = 55,99%). The activating solution used in GBFS/OPC concrete featured a solution module (Ms = SiO_2/Na_2O) of 1 and was incorporated in a proportion of 5% of Na_2O according to slag content. In the case of the binary system (FA/GBFS), the components of the mixture were dosed to obtain molar ratios of Si/Al: 3,85 and Na/Si: 0,25. In this mix, the activator moduli Ms was 1,55. The proportions used in FA/GBFS were determined in previous studies (Valencia-Saavedra, Mejia de Gutiérrez and Gordillo, 2018). To prepare the concretes, river sand with a fineness modulus of 3,16 and crushed gravel with a maximum particle size of 12,7 mm were used according to ASTM C39 standards (ASTM International, 2018). The mix design was carried out according to the recommendations of ACI 211 Committee (2009).

Table 2 shows the proportions of the materials for each of the produced concretes. The selected slump was between 50 and 180 mm, in order to maintain medium consistency (plastic) for the manufactured concrete, which is ideal for handmade placements and reinforced sections. Then, the concrete specimens were kept for the first 24 hours in metallic molds under relative humidity (>90%), at room temperature (24 °C), and covered with wet foams. Subsequently, the alkali-activated concrete specimens were removed from the molds and cured in a wet chamber (90% R.H. and 24 °C) up to the test ages. OPC and GBFS/OPC* 80/20 samples were submerged and cured in water (100% R.H.).

Experimental tests

The compressive strength test was carried out on cylindrical samples (76,2 mm diameter x 152,4 mm height) as specified by ASTM C109 (ASTM International, 2016). The measurements of compressive strength were conducted at 7, 28, 180, and 360 days of curing, using three (3) samples for each mixture and test age.

Table 2. Design of mixtures and properties in the fresh state of the concretes

Component proportions, kg/m^3	Concrete Mixes			
	OPC	GBFS/OPC*	GBFS/OPC	FA/GBFS
Cement	400	80	80	–
FA	–	–	–	320
GBFS	–	320	320	80
SS	–	–	44,6	158,4
NaOH	–	–	12,2	28,6
Fine aggregate	972,7	989,9	989,9	972,7
Coarse Aggregate	704,4	716,9	716,9	704,4
L/S ratio	0,48	0,48	0,48	0,48
Slump (mm)	60	50	70	180

Source: Authors

To measure the water absorption capacity of each mixture (capillary sorption), two cylindrical samples (76,2 mm diameter and 76,2 mm height) were used per evaluated mixture, according to the Swiss Standard SIA 162/1 (EMPA, 1989). After 28 days of curing, the samples were dried in a

furnace at 60 °C for 48 hours until a constant weight achieved. Then, the lateral surface of each cylinder was covered with waterproof paint. The samples were placed on a tray in a sealed container, in such a way that the lower surface was in contact with the water up to a height of 5 mm, allowing the water to enter through it. At different times, the samples were removed from the container and weighed to evaluate the weight gain. The kinetics of water absorption in concrete can be described approximately by the coefficients: *Water absorption coefficient* $-K$ ($Kg/m^2s^{1/2}$) and *Resistance to water penetration* $-m$ (s/m^2). K corresponds to the initial slope of the sorptivity plot (water absorption expressed as Kg/m^2 versus the square root of time in $s^{1/2}$). The value of "m" is calculated using Equation (1):

$$m = t/Z^2 \quad (1)$$

where t is the saturation time of the sample, and Z is the height of the evaluated sample.

The concrete's resistance to chloride ion penetration was evaluated by determining the charge passed through the concrete, as specified by ASTM C1202 (ASTM International, 2019a). After 28 days of curing, two 50-mm-long disks were cut from the middle segment of the manufactured cylinders. Specimens with diameters of 76,2 mm were used. The samples were conditioned according to the procedure mentioned in the standard and then placed in the test cell. One side was in contact with a 3,5% NaCl solution, and the other one, with a saturated solution of calcium hydroxide ($Ca(OH)_2$). Direct current (DC) at 60 V was applied, and the current flow was recorded in 5-minute intervals to cover a period of 6 hours. It is noted that this methodology is used to evaluate chloride permeability in concretes based on OPC; there is no standard method for alkali-activated materials.

In addition, the resulting hydration products were characterized using X-ray diffraction techniques on a PanAnalytical X'Pert MRD diffractometer with Cu Ka radiation and a step size of 0,020° in a range between 5 and 60° 2θ. Microstructural characterisation was conducted by scanning electron microscopy (SEM) using a JEOL JSM-6490LV high-vacuum device (3 x 10^{-6} Torr) at an acceleration voltage of 20 keV.

Results and discussion

Compressive strength

Figure 2 shows the average compressive strength values with respect to the curing age of the different concretes that were evaluated in this study, namely, reference concretes (non-activated binders) (OPC and GBFS/OPC*) and alkali-activated concretes, GBFS/OPC-AA and FA/GBFS-AA.

As expected, gain in mechanical compressive strength from 7 to 360 days of curing is observed for all the evaluated mixtures (Figure 2). The strength gains of the AA concretes between 7 and 28 days of curing were 30,17% for GBFS/OPC, and 23,51% for FA/GBFS. The alkali-activated concretes GBFS/OPC 80/20-AA and FA/GBFS-AA exhibited a similar strength gain (43%) between 28 and 360 days of curing. It should be noted

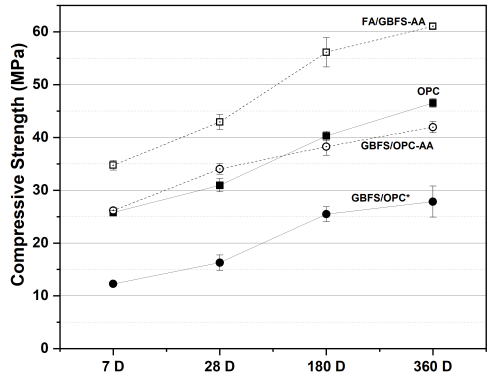

Figure 2. Compressive strength of the OPC and alkaline activated (GBFS/OPC and FA/GBFS) concretes.
Source: Authors

that the FA/GBFS alkali-activated concrete presented the best compressive strength: 43 and 61 MPa at 28 and 360 days of curing, respectively. This behaviour of the FA/GBFS 80/20 concrete, which was not appreciable in samples with 100% FA (Valencia-Saavedra, Mejia de Gutiérrez and Gordillo, 2018), can be attributed to the presence of the blast furnace slag, a material that provides calcium to the system, generating hydrated calcium silicate gel as reaction product, in addition to the aluminosilicate gels proper to the alkaline activation of fly ash (C-A-S-H/N-A-S-H). This performance agrees with those reported by other authors (Manjunatha et al., 2014; Gopalakrishnan and Chinnaraju, 2019; Nath and Kumar, 2014). At 7 and 28 days for FA/GBFS concretes (80/20) designed with 400 kg/m^3 of precursor, Nath and Kumar (2014) reported compressive strength values similar to those obtained in the present study, although the proportions of activator and the characteristics of fly ash were different. On the contrary, Chi (2016) reported a compressive strength lower than 20 MPa at 28 days using a FA/GBFS ratio of 75/25 concrete specimens. The addition of GBFS as a partial replacement of fly ash contributes to the material hardening at room temperature and to develop greater strength at early and longer ages. Additionally, the presence of the two gels (C-A-S-H and N-A-S- H) produces a significantly more compact microstructure than the one generated by OPC cement paste (Chotetanorm, Chindaprasirt, Sata, Rukzon and Sathonsaowaphak, 2013; Deb, Nath and Sarker, 2014; Marjanović, Komljenović, Baščarević, Nikolić and Petrović, 2015; Ryu, Lee, Koh and Chung, 2013, Ismail et al., 2014). In conclusion, the coexistence and interaction between N-A-S-H and C-A-S-H gels generate a higher degree of cross-linking within the reaction products.

The blended GBFS/OPC* 80/20, compared to OPC concrete, displays a significantly reduced compressive strength, especially at early ages: 12 MPa at 7 days. The early performance of the GGBS/OPC binder is poor because the hydration of GGBS needs the presence of calcium hydroxide ($Ca(OH)_2$), which is formed through the hydration of OPC (Angulo-Ramírez, D. E., Mejía de Gutiérrez, R., and Puertas, F., 2017). On the contrary, when this material is alkali-activated (GBFS/OPC-AA), its resistance increases up to 110% at 7 days

of curing. At greater ages (180, 360 days), the increase was up to 50%. The mechanical development of GBFS/OPC-AA was comparable to that reported by OPC concrete. Amer, Kohail, El-Feky, Rashad, and Khalaf (2020), using the Taguchi method, reported that the optimum GBFS/OPC ratio and solution modulus (Ms) were 80/20 and 1,0, coinciding with the proportions used in this study. However, the authors used Na_2O = 10%, which is two times higher than what was used in this study (5%). The performance of an alkali-activated GGBS/OPC binder with GGBS content of 70 to 100 wt%, cured at temperatures of 20, −5, and −20 °C, was studied by Zhang, Yang, Ju, and Yang (2020). The highest compressive strength was achieved when the GGBS content was 80 wt% (62,7 MPa in 28 days at −5 °C). The authors suggest that this type of binder can be an environment-friendly cementitious material for winter construction. These recent results show an opportunity to use these materials at low temperature conditions, where the hydration processes of conventional cements can be slow.

Microstructural analyses of activated alkali systems performed by X-ray diffraction and electron microscopy (SEM) confirmed the presence of C-A-S-H/N-A-S-H gels and the densification of the generated microstructures. The X-ray diffractograms, after 28 days of normal curing of the FA/GBFS and GBFS/OPC systems are presented in Figure 3. The presence of the crystalline phases associated with the original materials, which were not affected by the alkaline solutions, was observed (Mejía, Rodríguez, and Mejía de Gutiérrez, 2014). Hydration products such as gehlenite, hydrotalcite, and a crystalline portion of C-S-H gel were identified in the GBFS/OPC system, the latter of which was also found in the diffractogram of the FA/GBFS system. For both systems, the peak located at approximately 30° 2θ is attributable to the main phase C-(A)-S-H, which overlaps with that of calcite. A crystalline phase of sodium aluminosilicates (analcime, $NaAlSi_2O_6H_2O$) was also identified, thus confirming the presence of a NASH-type binding gel in the FA/GBFS system.

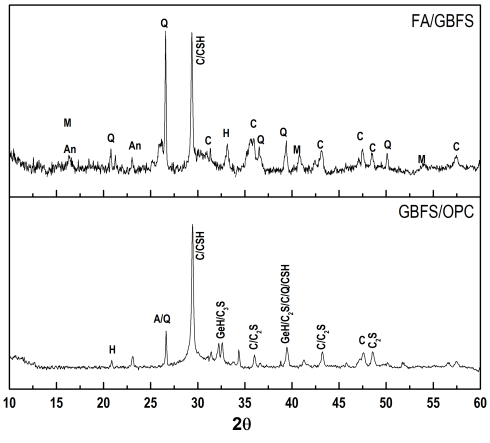

Figure 3. X-ray diffractograms of the FA/GBFS and GBFS/OPC-AA systems. A: Aragonite; C: Calcite; H: Hydrotalcite; GeH: Hydrated gehlenite (C_2ASH_8/C_4AH_{13}); Y: Gypsum; Q: Quartz; M: Mullite; An: Analcime; H: Hematite.
Source: Authors

Figure 4 shows the microstructures observed by SEM for the tested concretes. A good paste-aggregate adhesion can be seen in the activated materials, in addition to a highly dense microstructure, which is related to the favorable mechanical properties that were obtained. This feature is also related to the increased tortuosity within the structures of these systems, which contributes to their greater resistance to the penetration of water and aggressive agents such as chloride ions seen in the evaluation of physical properties.

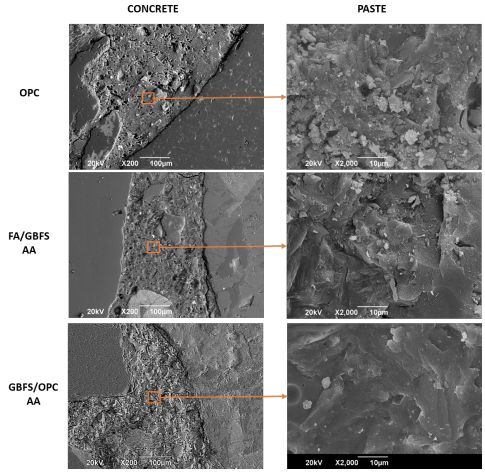

Figure 4. Microstructure of the FA/GBFS and GBFS/OPC alkali-activated concrete (left) and paste (right) systems observed by scanning electron microscopy.
Source: Authors

Physical properties

Table 3 shows the results of the water absorption test based on capillary action for the concretes, which were evaluated after 28 days of curing, where "k" represents the absorption coefficient and 'm' the resistance to water penetration. The results show that the alkali-activated concretes GBFS/OPC and FA/GBFS, featured lower absorption coefficients (52% and 10%, respectively) compared to 100% OPC. These concretes also exhibited a greater resistance to water penetration, with values of 33% and 71%, respectively, compared to conventional OPC.

Table 3. Capillary absorption properties of concretes (*without alkali-activation)

CONCRETE MIX	OPC	GBFS/OPC*	GBFS/OPC	FA/GBFS
k (kg/m^2.seg$^{1/2}$)	0,0292	0,0190	0,0140	0,0262
m*10^7 (s/m^2)	1,89	2,51	2,51	3,24

Source: Authors

Wardhono, Gunasekara, Law and Setunge (2017) found significant differences between the water permeated by concretes based on FA and GBFS. However, in the case of FA/GBFS compared to the 100% OPC, the reduction is attributed to the sodium aluminosilicate gels that are generated during the geopolymerisation process. This gel fills the spaces and interfaces formed between the paste

and aggregates, thereby reducing the porous structure, and generating a denser microstructure, as previously evinced. The greater resistance to water penetration presented by the alkali-activated concretes indicates the refinement of pores and an increase in the tortuosity of the pore network in this system. In general, the coexistence of C-A-S-H and N-A-S-H gels in FA/GBFS concrete explains the positive behavior of this material. The best characteristics presented by GBFS/OPC and FA/GBFS are related to the greater densification and compactness observed in the SEM test, and due to the lower number of capillaries or permeable pores present in this type of alkaline-activated materials (Valencia-Saavedra et al., 2018; Chotetanorm et al., 2013; Qureshi and Ghosh, 2014; Aydin and Baradan, 2014).

Figure 5 shows the results of the rapid chloride permeability test, performed on OPC, GBFS/OPC, and FA/GBFS concretes after 28 days of curing, based on the procedure described in ASTM C1202 (ASTM International, 2019a). From the results obtained in this study, it can be deduced that the chloride resistance in the evaluated AA concretes is higher than in OPC. According to the criteria defined in the ASTM standard, the penetrability of the chloride ion in OPC can be classified as moderate, unlike the concretes with alkaline activation, which showed low penetrability in the case of FA/GBFS and very low penetrability for GBFS/OPC. This finding agrees with the studies of Bernal, Mejía de Gutiérrez and Provis (2012) and Bernal, De Gutierrez, Delvasto, and Rodriguez (2010) who investigated 100% blast furnace slag alkaline-activated concretes and reported filtered load values below 1600 Coulomb. Likewise, Ismail et al. (2013) indicated a better behavior of the slag/fly ash concrete of alkaline activation and concluded that, in the presence of chlorides, these concretes feature lower chloride ion penetration and higher amounts of bound chlorides when compared with conventional OPC concrete. Yang, Yao and Zhang (2014) attributed this positive behavior of the FA/GBFS concrete to the incorporation of blast furnace slag as a precursor material, which contributes to the pore refinement within the structure, thus reducing the sorptivity and restricting the penetration of chloride ions, as was verified in the present study.

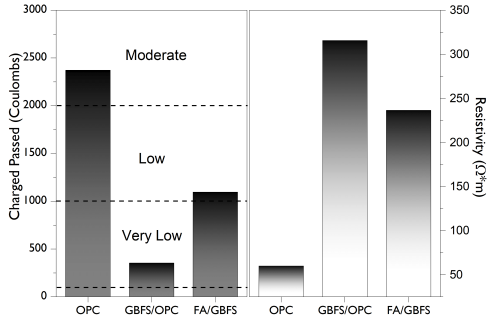

Figure 5. Rapid chloride permeability test of OPC and alkali-activated concretes FA/GBFS and GBFS/OPC: a) charge passed (Coulomb) b) resistivity of the concrete (Ω*m).
Source: Authors

Regarding the resistivity values calculated from the initial current results in this test, it was possible to notice increases in the alkaline-activated concretes of up to 5 times the value reported by OPC (Figure 5). The current results could be indicative of the concrete porosity. However, the connectivity, and tortuosity of the pore network and electric properties of concrete affected the results of this test. Therefore, the electrical conductivity of concrete depends on the pore solution, and the AA concretes present a high ionic concentration because of the presence of mobile cations such as Na+. For this reason, it is only possible to compare concretes with a similar pore solution chemistry (FA/GBFS and GBFS/OPC, both alkali-activated concretes) (Ismail et al., 2013). The highest electrical conductivity presented by the alkaline activated FA/GBFS, compared to the GBFS/OPC, could be attributed to the potentially high conductivity of the pore solution generated in this material, due to the high concentration of Na+ and OH- ions, present as a consequence of higher content of sodium silicate and sodium hydroxide in the mix (see Table 2) (Chi, 2012; Lloyd, Provis and van Deventer, 2010; Ravikumar and Neithalath, 2013). However, according to ASTM C1202, the results obtained of charge passed and resistivity of alkali-activated materials evaluated in the present study were consistent with each other (Figure 5).

It is important to note that this standard is specific for OPC-based materials and not for alkaline-activated materials, for which international standards have not yet been defined. This test has been controversial for the reasons described above, and therefore it urges the development of specific protocols for alkali-activated concretes (Ismail et al., 2013; Arbi Ghanmi, Nedeljković, Zuo and Ye, 2016). On the other hand, Thomas, Ariyachandra, Lezama and Peethamparan, 2018) studied different chloride permeability methods for AA concretes. They found that RCPT (ASTM C1202) results correlated very well with diffusion coefficients from salt ponding tests according ASTM C1543 (ASTM International, 2010), unlike resistivity measurements with these results.

Conclusions

The results obtained in the present research led to the following conclusions:

The alkaline-activated FA/GBFS 80/20 has a better mechanical performance based on compression testing at ages up to 360 days of curing, in comparison with conventional 100% OPC concrete. The compressive strengths of FA/GBFS concrete were 34,75 MPa and 61,07 MPa at 7 and 360 days of curing, respectively, which are significant findings, considering the low-quality of the FA used. The alkali-activated blended concrete GBFS/OPC 80/20 presents a similar compressive strength to OPC: 26,15 MPa and 42 MPa at 7 and 360 days, respectively.

The alkali-activated concretes GBFS/OPC and FA/GBFS feature greater resistance to water penetration, 33 and 71% higher than those obtained in OPC. According to the results of permeability to the chloride ion, evaluated using the standard ASTM C1202 (ASTM International, 2019a), concretes FA/GBFS 80/20 and GBFS/OPC 80/20 could be

considered to have a low and very low permeablility, respectively.

Therefore, it is concluded that these two types of alkaline-activated concretes (FA/GBFS 80/20 and GBFS/OPC 80/20) have characteristics that are suitable for various applications in the construction sector, making them good alternative materials to Portland cement concrete.

Acknowledgements

This study was funded by the Colombian Institute for the Development of Science, Technology, and Innovation, COLCIENCIAS, (project: "Construction of prototype at the scale of rural housing using innovative materials with low carbon footprint", contract nr. 096-2016). The authors, who are members of the Composite Materials Group (GMC) from the Centre of Excellence in New Materials (CENM), would like to thank the Universidad del Valle (Cali, Colombia), at which the experimental work was carried out.

References

Abubakr, A. E., Soliman, A. M., and Diab, S. H. (2020). Effect of activator nature on the impact behaviour of Alkali-Activated slag mortar. *Construction and Building Materials*, *257*, 11953. 10.1016/j.conbuildmat.2020.119531

ACI Committee 211 (2009). *ACI 211.1 Standard Practice for Selecting Proportions for Normal, Heavyweight, and Mass* Concrete, Farmington Hills, Mi.: American Concrete Institute.

Aliabdo, A. A., El-Moaty, A., and Emam, M. (2019). Factors affecting the mechanical properties of alkali activated ground granulated blast furnace slag concrete. *Construction and Building Materials*, *197*, 339-355. 10.1016/J.conbuildmat.2018.11.086

Amer, I., Kohail, M., El-Feky, M.S., Rashad, and Khalaf M.A. (2020). Evaluation of using cement In Alkali-Activated Slag Concrete. *International Journal of Scientific & Technology Research, 9*(5) 245-248. https://www.researchgate.net/publication/342380210_Evaluation_Of_Using_Cement_In_Alkali-Activated_Slag_Concrete

Angulo-Ramírez, D. E., Mejía de Gutiérrez, R., and Puertas, F. (2017). Alkali-activated Portland blast-furnace slag cement: Mechanical properties and hydration. *Construction and Building Materials, 140*, 119-128. 10.1016/j.conbuildmat.2017.02.092

Arbi Ghanmi, K., Nedeljković, M., Zuo, Y., and Ye, G. (2016). *Durability of alkali-activated fly ash and slag concrete*. 9th International Concrete Conference: Environment, Efficiency and Economic Challenges for Concrete, Dundee, Scotland. https://repository.tudelft.nl/islandora/object/uuid%3A8f95eac7-4e66-4773-af05-802559652e0f

ASTM International (2019). *ASTM C618-19 Standard Specification for Coal Fly Ash and Raw or Calcined Natural Pozzolan for Use in Concrete*. West Conshohocken, PA: American Society for Testing and Materials. 10.1520/C0618-19

ASTM International (2016). *ASTM C109/C109M-16. Standard Test Method for Compressive Strength of Hydraulic Cement Mortars* (*Using 2-in. or [50-mm] Cube Specimens*. West Conshohocken, PA: American Society for Testing and Materials. 10.1520/C0109_C0109M-16A

ASTM International (2018). *ASTM C39/C39M-18 Standard Test Method for Compressive Strength of Cylindrical Concrete Specimens*. West Conshohocken, PA: American Society for Testing and Materials. 10.1520/C0039_C0039M-18

ASTM International (2019a). *ASTM C1202-19 Standard Test Method for Electrical Indication of Concrete's Ability to Resist Chloride Ion Penetration*. West Conshohocken, PA: American Society for Testing and Materials. 10.1520/C1202-19

ASTM International (2010). *ASTM C1543-10a Standard Test Method for Determining the Penetration of Chloride Ion into Concrete by Ponding* (Withdrawn 2019). West Conshohocken, PA: American Society for Testing and Materials. 10.1520/C1543-10A

Aydin, S. and Baradan, B. (2014). Effect of activator type and content on properties of alkali-activated slag mortars. *Composites Part B: Engineering*, *57*, 166-172. 10.1016/j.compositesb.2013.10.001

Bakharev, T., Sanjayan, J. G., and Cheng, Y.-B. (1999). Effect of elevated temperature curing on properties of alkali-activated slag concrete. *Cement and Concrete Research*, *29*(10), 1619-1625. 10.1016/S0008-8846(99)00143-X

Bernal, S. A., Mejía de Gutiérrez, R., and Provis, J. L. (2012). Engineering and durability properties of concretes based on alkali-activated granulated blast furnace slag/metakaolin blends. *Construction and Building Materials, 33*, 99-108. 10.1016/j.conbuildmat.2012.01.017

Bernal, S., De Gutierrez, R., Delvasto, S., and Rodriguez, E. (2010). Performance of an alkali-activated slag concrete reinforced with steel fibers. *Construction and Building Materials, 24*(2), 208-214. 10.1016/j.conbuildmat.2007.10.027

Bilim, C. and Atis, C.D. (2012). Alkali activation of mortars containing different replacement levels of ground granulated blast furnace slag. *Construction and Building Materials*, *28*(1), 708-712. 10.1016/j.conbuildmat.2011.10.018

Chi, M. (2012). Effects of dosage of alkali-activated solution and curing conditions on the properties and durability of alkali-activated slag concrete. *Construction and Building Materials, 35,* 240-245. 10.1016/j.conbuildmat.2012.04.005

Chi, M. (2016). Mechanical strength and durability of alkali-activated fly ash/slag concrete. *Journal of Marine Science and Technology, 24*(5), 958-967. 10.6119/JMST-016-0603-1

Chotetanorm, C., Chindaprasirt, P., Sata, V., Rukzon, S., and Sathonsaowaphak, A. (2013). High Calcium Bottom Ash Geopolymer: Sorptivity, Pore Size and Resistance to Sodium Sulfate Attack. *Journal of Materials in Civil Engineering*, *25*(1), 473. 10.1061/(ASCE)MT.1943-5533.0000560

Deb, P. S., Nath, P., and Sarker, P. K. (2014). The effects of ground granulated blast-furnace slag blending with fly ash and activator content on the workability and strength properties of geopolymer concrete cured at ambient temperature. *Materials and Design*, *62*, 32-39. 10.1016/j.matdes.2014.05.001

EMPA (1989). SIA 162/1 *Test No. 5 - Water Conductivity*. Zurich, Switzerland: Swiss Federal Laboratories for Materials Science and Technologies. http://shop.sia.ch/normenwerk/ingenieur/162-1_1989_d/D/Product

Gao, T., Shen, L., Shen, M., Liu, L., and Chen, F. (2016). Analysis of material flow and consumption in cement production process. *Journal of Cleaner Production, 112,* 553-565. 10.1016/j.jclepro.2015.08.054

Gartner, E. (2004). Industrially interesting approaches to "low-CO2" cements. *Cement and Concrete Research, 34*(9), 1489-1498. 10.1016/j.cemconres.2004.01.021

Gebregziabiher, B. S., Thomas, R., and Peethamparan, S. (2015). Very early-age reaction kinetics and microstructural development in alkali-activated slag. *Cement and Concrete Composites, 55,* 91-102. 10.1016/j.cemconcomp.2014.09.001

Gopalakrishnan, R., and Chinnaraju, K. (2019). Durability of ambient cured alumina silicate concrete based on slag/fly ash blends against sulfate environment. *Construction and Building Materials, 204,* 70-83. 10.1016/j.conbuildmat.2019.01.153

Hadjsadok, A., Kenai, S., Courard, L., Michel, F., and Khatib, J. (2012). Durability of mortar and concretes containing slag with low hydraulic activity. *Cement and Concrete Composites, 34*(5), 671-677. 10.1016/j.cemconcomp.2012.02.011

Ismail, I., Bernal, S. A., Provis, J. L., San Nicolas, R., Brice, D. G., Kilcullen, A. R., and van Deventer, J. S. J. (2013). Influence of fly ash on the water and chloride permeability of alkali-activated slag mortars and concretes. *Construction and Building Materials, 48,* 1187-1201. 10.1016/j.conbuildmat.2013.07.106

Ismail, I., Bernal, S. A., Provis, J. L., San Nicolas, R., Hamdan, S., and van Deventer, J. S. (2014). Modification of phase evolution in alkali-activated blast furnace slag by the incorporation of fly ash. *Cement Concrete Composites, 45,* 125-135. 10.1016/j.cemconcomp.2013.09.006

Juenger, M. C. G., Winnefeld, F., Provis, J. L., and Ideker, J. H. (2011). Advances in alternative cementitious binders. *Cement and Concrete Research, 41*(12), 1232-1243. 10.1016/j.cemconres.2010.11.012

Lloyd, R. R., Provis, J. L., and van Deventer, J. S. J. (2010). Pore solution composition and alkali diffusion in inorganic polymer cement. *Cement and Concrete Research, 40*(9), 1386-1392. 10.1016/j.cemconres.2010.04.008

Lübeck, A., Gastaldini, A.L.G., Barin, D.S., and Siqueira, H.C. (2012). Compressive strength and electrical properties of concrete with white Portland cement and blast-furnace slag. *Cement and Concrete Composites, 34*(3), 392-399. 10.1016/j.cemconcomp.2011.11.017

Manjunatha, G.S., Radhakrishna, Venugopal, K., and Maruthi, S.V. (2014). Strength Characteristics of Open Air Cured Geopolymer Concrete. *Transactions of the Indian Ceramic Society, 73*(2), 149-156. 10.1080/0371750X.2014.923330

Marjanović, N., Komljenović, M., Baščarević, Z., Nikolić, V., and Petrović, R. (2015). Physical–mechanical and microstructural properties of alkali-activated fly ash–blast furnace slag blends. *Ceramics International, 41*(1), 1421-1435. 10.1016/j.ceramint.2014.09.075

Mejía, J., Rodríguez, E. D., and Mejía de Gutiérrez, R. (2014). Utilización potencial de una ceniza volante de baja calidad como fuente de aluminosilicatos en la producción de geopolímeros. *Ingenieria y Universidad, 18*(2), 309. 10.11144/Javeriana.IYU18-2.upcv

Nath, P. and Kumar, P. (2014). Effect of GBFS on setting, workability and early strength properties of fly ash geopolymer concrete cured in ambient condition. *Construction and Building Materials*, *66*, 163-171. 10.1016/j.conbuildmat.2014.05.080

Noorliyana, H.A., Al Bakri, A.M.M., Azira, M.., Mariamadzliza, M.N, Kamrosni, A.., and Kamarudin, H. (2013). Alkali Activated Blast-Furnace Slag Cement: The Opportunity to Solve Sustainable Issues. *Advances in Environmental Biology, 7*(12), 3713-3715.

Pacheco-Torgal, F., Castro-Gomes, J., and Jalali, S. (2008a). Alkali-activated binders: A review: Part 1. Historical background, terminology, reaction mechanisms and hydration products. *Construction and Building Materials, 22*(7), 1305-1314. 10.1016/j.conbuildmat.2007.10.015

Pacheco-Torgal, F., Castro-Gomes, J., and Jalali, S. (2008b). Alkali-activated binders: A review. Part 2. About materials and binders manufacture. *Construction and Building Materials, 22*(7), 1315-1322. 10.1016/j.conbuildmat.2007.03.019

Pal, S. C., Mukherjee, A., and Pathak, S. R. (2003). Investigation of hydraulic activity of ground granulated blast furnace slag in concrete. *Cement and Concrete Research*, *33*(9), 1481-1486. 10.1016/S0008-8846(03)00062-0

Pereira, A., Akasaki, J. L., Melges, J. L. P., Tashima, M. M., Soriano, L., Borrachero, M. V., and Payá, J. (2015). Mechanical and durability properties of alkali-activated mortar based on sugarcane bagasse ash and blast furnace slag. *Ceramics International, 41*(10), 13012-13024. 10.1016/j.ceramint.2015.07.001

Puertas, F. (1993). Escorias de alto horno: composición y comportamiento hidráulico. *Materiales de Construcción, 43*(229), 37-8. 10.3989/mc.1993.v43.i229.687

Puertas, F., González-Fonteboa, B., González-Taboada, I., Alonso, M.M., Torres-Carrasco, M., Rojo, G., and Martínez-Abella, F. (2018). Alkali-activated slag concrete: Fresh and hardened behavior. *Cement and Concrete Composites*, *85*, 22-31. 10.1016/j.cemconcomp.2017.10.003

Qu, B., Martin, A., Pastor, J. Y., Palomo, A., and Fernández-Jiménez, A. (2016). Characterisation of pre-industrial hybrid cement and effect of pre-curing temperature. *Cement and Concrete Composites*, *73*, 281-288. 10.1016/j.cemconcomp.2016.07.019

Qureshi, M. N., and Ghosh, S. (2014). Effect of Silicate Content on the Properties of Alkali-Activated Blast Furnace Slag Paste. *Arabian Journal for Science and Engineering, 39*(8), 5905-5916. 10.1007/s13369-014-1172-x

Rashad, A. M. (2013). A comprehensive overview about the influence of different additives on the properties of alkali-activated slag – A guide for Civil Engineer. *Construction and Building Materials, 47*, 29-55. 10.1016/j.conbuildmat.2013.04.011

Ravikumar, D. and Neithalath, N. (2013). Electrically induced chloride ion transport in alkali activated slag concretes and the influence of microstructure. *Cement and Concrete Research, 47*, 31-42. 10.1016/j.cemconres.2013.01.007

Reddy, D. V., Edouard, J. B., Sobhan, K., and Tipnis, A. (2011). *Experimental evaluation of the durability of fly ash-based geopolymer concrete in the marine environment*. Ninth LACCEI Latin American and Caribbean Conference (LACCEI'2011), Engineering for a Smart Planet, Innovation, Information Technology and Computational Tools for Sustainable Development, Medellín, Colombia. https://pdfs.semanticscholar.org/7ebc/7c3101f667784eb48baa1e4d955051bd514c.pdf

Robayo, R. A., Mulford, A., Munera, J., and Mejía de Gutiérrez, R. (2016). Alternative cements based on alkali-activated red clay brick waste. *Construction and Building Materials, 128,* 163-169. 10.1016/j.conbuildmat.2016.10.023

Ryu, G. S., Lee, Y. B., Koh, K. T., and Chung, Y. S. (2013). The mechanical properties of fly ash-based geopolymer concrete with alkaline activators. *Construction and Building Materials, 47,* 409-418. 10.1016/j.conbuildmat.2013.05.069

Tänzer, R., Buchwald, A., and Stephan, D. (2015). Effect of slag chemistry on the hydration of alkali-activated blast-furnace slag. *Materials and Structures, 48*(3), 629-641. 10.1617/s11527-014-0461-x

Taylor, M., Tam, C., and Gielen, D. (2006). Energy efficiency and CO2 emissions from the global cement industry. *IEA-WBCSD Workshop*, Paris. https://www.researchgate.net/publication/237232402_Energy_Efficiency_and_CO2_Emissions_from_the_Global_Cement_Industry

Tennakoon, C., Shayan, A., Sanjayan, J. G., and Xu, A. (2017). Chloride ingress and steel corrosion in geopolymer concrete based on long term tests. *Materials and Design*, *116*, 287-299. 10.1016/j.matdes.2016.12.030

Thomas, R. J., Ariyachandra, E., Lezama, D., and Peethamparan, S. (2018). Comparison of chloride permeability methods for Alkali-Activated concrete. *Construction and Building Materials, 165*, 104-111. 10.1016/j.conbuildmat.2018.01.016

Valencia Saavedra, W. G., Angulo, D. E., and Mejía de Gutiérrez, R. (2016). Fly Ash Slag Geopolymer Concrete: Resistance to Sodium and Magnesium Sulfate Attack. *Journal of Materials in Civil Engineering*, *28*(12), 04016148. 10.1061/(ASCE)MT.1943-5533.0001618

Valencia-Saavedra, W., Mejía de Gutiérrez, R., and Gordillo, M. (2018). Geopolymeric concretes based on fly ash with high unburned content. *Construction and Building Materials*, *165*, 697-706. 10.1016/j.conbuildmat.2018.01.071

Valencia-Saavedra, W.G. and Mejía de Gutiérrez, R. (2017). Performance of geopolymer concrete composed of fly ash after exposure to elevated temperatures. *Construction and Building Materials*, *154*, 229-235. 10.1016/j.conbuildmat.2017.07.208

Valencia-Saavedra, W.G., Mejia de Gutiérrez, R., and Puertas, F. (2020). Performance of FA-based geopolymer concretes exposed to acetic and sulfuric acids. *Construction and Building Materials, 257*, 119503. 10.1016/j.conbuildmat.2020.119503

Wardhono, A., Gunasekara, C., Law, D. W., and Setunge, S. (2017). Comparison of long-term performance between alkali activated slag and fly ash geopolymer concretes. *Construction and Building Materials*, *143*, 272-279. 10.1016/j.conbuildmat.2017.03.153

Weil, M., Dombrowski, K., and Buchawald, A. (2009). Life cycle analysis of geopolymers. In J. L. Provis and J. S. J. Van Deventer (Eds.), *Geopolymers: structures, processing, properties and industrial applications* (pp. 194-210). Cambridge, UK: Woodhead Publishing Series in Civil and Structural Engineering. 10.1533/9781845696382.2.194

Yang, T., Yao, X., and Zhang, Z. (2014). Quantification of chloride diffusion in fly ash–slag-based geopolymers by X-ray fluorescence (XRF). *Construction and Building Materials*, *69*, 109-115. 10.1016/j.conbuildmat.2014.07.031

Zhang, G., Yang, H., Ju, Ch., and Yang Y. (2020). Novel selection of environment-friendly cementitious materials for winter construction: Alkali-activated slag/Portland cement. Journal of Cleaner Production 258, 120592. 10.1016/j.jclepro.2020.120592

Zhang, C.-Y., Han, R., Yu, B., and Wei, Y.-M. (2018). Accounting process-related CO2 emissions from global cement production under Shared Socioeconomic Pathways. *Journal of Cleaner Production*, *184,* 451-465. 10.1016/j.jclepro.2018.02.284